A NEW DATA-AIDED CARRIER FREQUENCY OFFSET ESTIMATION ALGORITHM FOR OFDM SYSTEMS

Amine Laourine[1], *Alex Stéphenne*[1,2] *and Sofiène Affes*[1]

[1] INRS-EMT, 800, de la Gauchetière Ouest, Bureau 6900, Montreal, H5A 1K6
[2] Ericsson Canada, 8400, Decarie Blvd, Montreal, H4P 2N2
Emails: laourine@emt.inrs.ca, stephenne@ieee.org, affes@emt.inrs.ca

ABSTRACT

This paper proposes a new data-aided Carrier Frequency Offset (CFO) estimation scheme for OFDM communications suitable for frequency-selective fading channels. The proposed method is based on the transmission of a specially designed synchronization symbol that creates a particular signal structure between the received observation samples at the receiver. This structure is exploited to derive a very accurate Maximum Likelihood (ML) CFO estimator. To reduce the estimation complexity, a simplified version with lower computational load is derived which exhibits only a moderate loss in accuracy. This simplified version could typically be employed in the acquisition phase while the original version would allow for a very accurate subsequent tracking phase. Simulations over frequency-selective fading channels confirm the superiority of the proposed method compared to most recent algorithms presented in the literature.

1. INTRODUCTION

Orthogonal Frequency Division Multiplexing (OFDM) performance is highly impaired by frequency offsets [1]. The carrier frequency offset (CFO) should therefore be estimated and compensated before demodulating the data with the Discrete Fourier Transform (DFT). Several data-aided schemes of frequency offset estimation in OFDM systems have been investigated. These methods are based on the cyclic transmission of known data blocks (or training sequences) that allows for the estimation of the CFO from the estimation of the phase rotation between these blocks at the receiver [2]-[5]. In [2], the authors used two training symbols. The first one has two identical halves in the time domain and corrects the carrier frequency offset that lies within the subcarrier spacing. The second compensates the integer part of the carrier frequency offset. An improvement of this method was presented in [3]. A 50% overhead reduction is reached there by sending a unique training symbol having L identical segments, thereby offering an acquisition range of $\pm L/2$ the subcarrier spacing. A training symbol having the same structure was recently used differently in [4] to achieve a higher accuracy. More recently, a new synchronization symbol proposed in [5] allowed for performance gains over Schmidl's algorithm [2].

In this paper we propose a new synchronization symbol structure and a new CFO estimator that outperforms the previous techniques in accuracy. Based on the original shape of the new synchronization symbol, the ML-based CFO estimator is derived, providing high accuracy without involving a high computational load. Our method has an acquisition range that can reach $\pm N/2p$ the subcarrier spacing, where p is a user-selected parameter characterizing our synchronization symbol and N is the number of OFDM subcarriers. As supported by simulations, our algorithm provides higher accuracy compared to the previously cited methods.
The paper is organized as follows. In Section 2, the OFDM system model is described. The designed synchronization symbol and the ML-based CFO estimator are presented in Section 3. Numerical examples are illustrated in Section 4. Conclusions are given in Section 5.

2. SYSTEM MODEL

We consider a discrete-time OFDM system with N subcarriers. At the transmitter, N complex-valued symbols X_k, that belong to a QAM or PSK constellation, modulate N orthogonal subcarriers using the Inverse Fast Fourier Transform (IFFT). Before transmission, a cyclic prefix is appended at the beginning of the signal, yielding:

$$s(n) = \begin{cases} x(n+N), & \text{if } -N_g \leq n < 0, \\ x(n), & \text{if } 0 \leq n \leq N-1, \end{cases}$$

where $x(n) = \frac{1}{N}\sum_{k=0}^{N-1} X_k e^{\frac{j2\pi kn}{N}}, n = 0, \ldots, N-1$. At the receiver, the cyclic prefix is discarded leading to the following received samples:

$$\begin{aligned} r(n) &= \sum_{l=0}^{N_c-1} h_l s(n-l) e^{\frac{j2\pi\varepsilon n}{N}} + w(n) \qquad (1) \\ &= \frac{e^{\frac{j2\pi n\varepsilon}{N}}}{N} \sum_{l=0}^{N_c-1} h_l \Big(\sum_{k=0}^{N-1} X_k e^{\frac{j2\pi k(n-l)}{N}}\Big) + w(n) \end{aligned}$$

$$r(n) = \frac{1}{N} e^{j2\pi n\varepsilon/N} \sum_{k=0}^{N-1} X_k H_k e^{j2\pi kn/N} + w(n)$$
$$= y(n) + w(n), \quad n = 0, \ldots, N-1, \tag{2}$$

where $H_k = \sum_{l=0}^{N_c-1} h_l e^{-j2\pi kl/N}$ is the transfer function of the channel at the frequency of the kth subcarrier, N_c corresponds to the channel length, ε is the relative carrier frequency offset (the ratio of the actual frequency offset to the intercarrier spacing), and $w(n)$ is an additive complex white Gaussian noise with variance σ^2.

3. CFO ESTIMATION

To estimate the CFO, we propose to periodically transmit the following synchronization symbol:

$$X_{k+1} = e^{j2\pi pk/N} X_k, \quad k = 0, \ldots, N-2, \tag{3}$$

where p is a user-selected integer such that $1 \leq p \leq N-1$. Based on the special structure of this synchronization symbol, we will prove that there is a relationship between $r(n)$ and $r(n+p)$ that will allow us to easily derive the maximum likelihood estimator of the CFO. First, let us consider the noiseless part of $r(n+p)$:

$$y(n+p) = \frac{e^{\frac{j2\pi(n+p)\varepsilon}{N}}}{N} \sum_{k=0}^{N-1} X_k H_k e^{\frac{j2\pi k(n+p)}{N}} \tag{4}$$
$$= \frac{e^{\frac{j2\pi(n+p)\varepsilon}{N}}}{N} \sum_{k=0}^{N-1} H_k e^{\frac{j2\pi kn}{N}} X_k e^{\frac{j2\pi kp}{N}} \tag{5}$$
$$= \frac{e^{\frac{j2\pi(n+p)\varepsilon}{N}}}{N} \left[\sum_{k=0}^{N-2} H_k e^{\frac{j2\pi kn}{N}} X_{k+1} \right. \tag{6}$$
$$\left. + \; H_{N-1} e^{\frac{j2\pi(N-1)n}{N}} X_{N-1} e^{\frac{j2\pi p(N-1)}{N}} \right]$$
$$= \frac{e^{\frac{j2\pi(n+p)\varepsilon}{N}}}{N} \left[\sum_{k=1}^{N-1} H_{k-1} e^{\frac{j2\pi(k-1)n}{N}} X_k \right. \tag{7}$$
$$\left. + \; H_{N-1} e^{-\frac{j2\pi n}{N}} X_{N-1} e^{\frac{j2\pi p(N-1)}{N}} \right]$$
$$= \frac{e^{\frac{j2\pi[(n+p)\varepsilon-n]}{N}}}{N} \left[\sum_{k=1}^{N-1} H_{k-1} e^{\frac{j2\pi kn}{N}} X_k \right. \tag{8}$$
$$\left. + \; H_{N-1} X_{N-1} e^{\frac{j2\pi p(N-1)}{N}} \right].$$

In a system with many subcarriers, the inequality $N_c \ll N$ is always fulfilled. In this case, $H_k \approx H_{k-1}$ for $k = 1, \ldots, N-1$ and $H_{N-1} \approx H_0$, which is equivalent to saying that adjacent subcarriers experience approximately the same channel, therefore:

$$y(n+p) \simeq e^{j2\pi[(n+p)\varepsilon-n]/N} \frac{1}{N} [\sum_{k=1}^{N-1} H_k e^{j2\pi kn/N} X_k$$
$$+ \; H_0 X_{N-1} e^{j2\pi p(N-1)/N}]. \tag{9}$$

The second term $X_{N-1} e^{j2\pi p(N-1)/N}$ could be further developed:

$$X_{N-1} e^{j2\pi p(N-1)/N} = e^{j2\pi p(N-1)/N} X_0 \prod_{k=0}^{N-2} e^{j2\pi pk/N}$$
$$= X_0 \prod_{k=0}^{N-1} e^{\frac{j2\pi pk}{N}} = X_0 e^{j2\pi \frac{p\sum_{k=0}^{N-1} k}{N}}$$
$$= X_0 e^{j2\pi \frac{pN(N-1)}{2N}}$$
$$= X_0 e^{j\pi p(N-1)}. \tag{10}$$

As N is usually a power of 2, then:

$$X_{N-1} e^{j2\pi p(N-1)/N} = \begin{cases} X_0, & \text{if } p \text{ is even,} \\ -X_0, & \text{if } p \text{ is odd.} \end{cases}$$

Subsequently we have:

$$y(n+p) \simeq \begin{cases} e^{j2\pi[p\varepsilon-n]/N} y(n), \text{if } p \text{ is even,} \\ e^{j2\pi[p\varepsilon-n]/N} y(n) - \\ 2e^{j2\pi[(n+p)\varepsilon-n]/N} \frac{1}{N} X_0 H_0, \text{if } p \text{ is odd.} \end{cases}$$

Since usually $N \gg 1$, then whether the parameter p is odd or even, we have:

$$y(n+p) \approx e^{j2\pi[p\varepsilon-n]/N} y(n). \tag{11}$$

Based on this last equation, we can now state that:

$$r(n+p) = y(n+p) + w(n+p)$$
$$\approx e^{j2\pi[\varepsilon p-n]/N} y(n) + w(n+p). \tag{12}$$

Finally, we have the following set of equations:

$$r(n+p) \approx e^{j2\pi[\varepsilon p-n]/N} y(n) + w(n+p)$$
$$r(n) = y(n) + w(n), \tag{13}$$

where $n \in \{0, \ldots, N-p-1\}$. The previous equation can be rewritten as follows:

$$\mathbf{R}_1 \approx \mathbf{Y}_0 \mathbf{\Xi}(\varepsilon) + \mathbf{W}_1$$
$$\mathbf{R}_0 = \mathbf{Y}_0 + \mathbf{W}_0 \tag{14}$$

where the following notations have been adopted:

$$\mathbf{Y}_0 = [y(0), y(1), \ldots, y(N-p-1)];$$
$$\mathbf{R}_i = [r(ip), \ldots, r(ip+N-p-1)], \; for \; i = 0, 1;$$
$$\mathbf{W}_i = [w(ip), \ldots, w(ip+N-p-1)], \; for \; i = 0, 1;$$
$$\mathbf{\Xi}(\varepsilon) = e^{j2\pi p\varepsilon/N} diag(1, e^{-j2\pi/N}, \ldots, e^{-j2\pi(N-p-1)/N})$$
$$= e^{j2\pi p\varepsilon/N} \mathbf{E}.$$

Equation (14) leads to:

$$\begin{aligned}\mathbf{R}_1 &\approx (\mathbf{R}_0 - \mathbf{W}_0)\mathbf{\Xi}(\varepsilon) + \mathbf{W}_1 \\ &\approx \mathbf{R}_0\mathbf{\Xi}(\varepsilon) + \mathbf{W}_1 - \mathbf{W}_0\mathbf{\Xi}(\varepsilon). \end{aligned} \quad (15)$$

The special shape of the synchronization symbol has generated a structure in the received samples that will facilitate the estimation of the CFO. The Maximum Likelihood (ML) estimate of ε is simply the following:

$$\hat{\varepsilon} = \arg\max_{\varepsilon}[f(\mathbf{R}_1|\mathbf{R}_0, \varepsilon)], \quad (16)$$

where f is the Likelihood function. Since the noise samples $w(i)$ are white Gaussian with zero mean, then $\mathbf{W}_1$ and $\mathbf{W}_0$ are also zero-mean white Gaussian vectors. Hence f is a multivariate Gaussian CDF with mean vector $\mathbf{R}_0\mathbf{\Xi}(\varepsilon)$ and a covariance matrix

$$\mathbf{\Sigma} = E[(\mathbf{W}_1 - \mathbf{W}_0\mathbf{\Xi}(\varepsilon))^H(\mathbf{W}_1 - \mathbf{W}_0\mathbf{\Xi}(\varepsilon))], \quad (17)$$

where the superscript H denotes the conjugate transpose. This last equation can be further developed:

$$\begin{aligned}\mathbf{\Sigma} &= E[\mathbf{W}_1^H\mathbf{W}_1] + \mathbf{\Xi}(\varepsilon)^H E[\mathbf{W}_0^H\mathbf{W}_0]\mathbf{\Xi}(\varepsilon) \\ &- E[\mathbf{W}_1^H\mathbf{W}_0]\mathbf{\Xi}(\varepsilon) - \mathbf{\Xi}(\varepsilon)^H E[\mathbf{W}_0^H\mathbf{W}_1]. \end{aligned} \quad (18)$$

Noting, however, that $E[\mathbf{W}_1^H\mathbf{W}_1] = E[\mathbf{W}_0^H\mathbf{W}_0] = \sigma^2\mathbf{I}_{N-p}$ and $\mathbf{\Xi}(\varepsilon)^H\mathbf{\Xi}(\varepsilon) = \mathbf{I}_{N-p}$, where $\mathbf{I}_{N-p}$ is the $(N-p)\times(N-p)$ identity matrix, we have:

$$\mathbf{\Sigma} = 2\sigma^2\mathbf{I}_{N-p} - E[\mathbf{W}_1^H\mathbf{W}_0]\mathbf{\Xi}(\varepsilon) - \mathbf{\Xi}(\varepsilon)^H E[\mathbf{W}_0^H\mathbf{W}_1]. \quad (19)$$

It can be also easily verified that:

$$\frac{1}{\sigma^2}E[\mathbf{W}_1^H\mathbf{W}_0] = \begin{cases} \mathbf{F}, \text{if } 1 \le p \le \frac{N}{2}, \\ \mathbf{0}_{(N-p)\times(N-p)}, \text{if } \frac{N}{2} \le p \le N-1, \end{cases}$$

where

$$\mathbf{F} \equiv \begin{bmatrix} \mathbf{0}_{(N-2p)\times p} & \mathbf{I}_{(N-2p)\times(N-2p)} \\ \mathbf{0}_{p\times p} & \mathbf{0}_{p\times(N-2p)} \end{bmatrix}. \quad (20)$$

Hence we have:

$$\hat{\varepsilon} = \arg\max_{\varepsilon}[f(\mathbf{R}_1|\mathbf{R}_0, \varepsilon)] = \arg\min_{\varepsilon}[J(\varepsilon)], \quad (21)$$

where

$$J(\varepsilon) = (\mathbf{R}_1 - \mathbf{R}_0\mathbf{\Xi}(\varepsilon))(\mathbf{I}_{N-p} - \mathbf{Q})^{-1}(\mathbf{R}_1 - \mathbf{R}_0\mathbf{\Xi}(\varepsilon))^H, \quad (22)$$

if $1 \le p \le \frac{N}{2}$, where $\mathbf{Q} = \frac{e^{j2\pi p\varepsilon/N}\mathbf{\Delta} + e^{-j2\pi p\varepsilon/N}\mathbf{\Delta}^H}{2}$ and $\mathbf{\Delta} = \mathbf{FE}$. For other values of p, i.e., $\frac{N}{2} \le p \le N-1$,

$$J(\varepsilon) = (\mathbf{R}_1 - \mathbf{R}_0\mathbf{\Xi}(\varepsilon))(\mathbf{R}_1 - \mathbf{R}_0\mathbf{\Xi}(\varepsilon))^H. \quad (23)$$

3.1. First estimator (ML)

Directly from (21), we can see that the CFO can be obtained by finding the value that minimizes $J(\varepsilon)$ over a given search grid. Since $J(\varepsilon)$ is periodic with period $\frac{N}{p}$ the acquisition range of the proposed algorithm is such that $|\varepsilon| \le \frac{N}{2p}$, which means that the search grid will cover this entire range. Finding the CFO this way can entail a high computational load. This complexity does not come from the inversion of the matrix $(\mathbf{I}_{N-p} - \mathbf{Q})$ since this matrix is sparse and it exhibits a shape similar to that of a tridiagonal matrix which is invertible by an algorithm with a reduced complexity $O(7(N-p))$ [6]. The complexity rather comes from the search of the minimum which is reached by evaluating $J(\varepsilon)$ over a large search grid.

Based on this last observation, we have decided to push further with our derivations. We will show that for $p \ge \frac{N}{2}$ a closed-form expression for $\hat{\varepsilon}$ can be obtained. For $p < \frac{N}{2}$, we will find a way to simplify the algorithm with only a small loss in accuracy, but with a huge gain in the computational load. This simplified version will be used as an acquisition algorithm. The non-simplified algorithm can be applied over a smaller search grid for fine tracking.

3.2. Second estimator (i.e., $p \ge \frac{N}{2}$)

By noting that $\mathbf{\Xi}(\varepsilon)\mathbf{\Xi}(\varepsilon)^H = \mathbf{I}_{N-p}$, we can easily prove the following relation:

$$\mathbf{\Xi}(\varepsilon)\frac{d\mathbf{\Xi}(\varepsilon)^H}{d\varepsilon} + \frac{d\mathbf{\Xi}(\varepsilon)}{d\varepsilon}\mathbf{\Xi}(\varepsilon)^H = \mathbf{0}. \quad (24)$$

And consequently, considering the case where $\frac{N}{2} \le p \le N-1$, it can be shown that

$$\frac{dJ(\varepsilon)}{d\varepsilon} = 0 \Rightarrow \hat{\varepsilon} = \frac{N}{4\pi p}\angle\left(\frac{\mathbf{R}_1\mathbf{E}^H\mathbf{R}_0^H}{\mathbf{R}_0\mathbf{E}\mathbf{R}_1^H}\right). \quad (25)$$

Equation (25) provides us with a closed-form expression of the CFO which is only optimal for $\frac{N}{2} \le p \le N-1$, i.e., this is the ML estimator when $p \ge \frac{N}{2}$. As it can be seen from Eq. (25) the acquisition range of this algorithm is $\pm\frac{N}{4p}$ the subcarrier spacing (half of the acquisition range of the first estimator).

3.3. Third estimator (i.e., $p < \frac{N}{2}$)

Assuming $1 \le p < \frac{N}{2}$, it is easy to verify that $\| \mathbf{Q} \|_2 \le \sqrt{\| \mathbf{Q} \|_1 \| \mathbf{Q} \|_\infty} \le \sqrt{1 \times 1}$. Moreover, we have established by observation that the value of $\| \mathbf{Q} \|_2$ rapidly decreases as p increases. If $\| \mathbf{Q} \|_2 < 1$, we can use the following formula:

$$(\mathbf{I}_{N-p} - \mathbf{Q})^{-1} = \sum_{k=0}^{\infty}\mathbf{Q}^k, \quad (26)$$

to establish the following approximation:

$$(\mathbf{I}_{N-p} - \mathbf{Q})^{-1} \approx \mathbf{I}_{N-p} + \mathbf{Q}. \quad (27)$$

This approximation will be more and more accurate as p increases until p exceeds $\frac{N}{2}-1$, at which point this approximation will become an equality as $\mathbf{Q}=\mathbf{0}$.

By replacing $(\mathbf{I}_{N-p}-\mathbf{Q})^{-1}$ with the last approximation in $J(\varepsilon)$, and by resolving the equation $\frac{dJ(\varepsilon)}{d\varepsilon}=0$, we find that $X=e^{j2\pi\hat{\varepsilon}p/N}$ is a root of the following polynomial:

$$\begin{aligned} P(X) &= (-\mathbf{R}_0\mathbf{E}\Delta\mathbf{R}_1^H)X^4+(-\mathbf{R}_0\mathbf{E}\mathbf{R}_1^H+\frac{\mathbf{R}_1\Delta\mathbf{R}_1^H}{2} \\ &+ \frac{\mathbf{R}_0\Omega\mathbf{R}_0^H}{2})X^3+(\mathbf{R}_1\mathbf{E}^H\mathbf{R}_0^H-\frac{\mathbf{R}_1\Delta^H\mathbf{R}_1^H}{2} \\ &+ \frac{\mathbf{R}_0\Omega^H\mathbf{R}_0^H}{2})X+\mathbf{R}_1\Delta^H\mathbf{E}^H\mathbf{R}_0^H, \end{aligned} \tag{28}$$

where $\Omega=\mathbf{EF}$. Hence, the problem of estimating the CFO amounts to that of finding the roots of a 4^{th} order polynomial, $P(X)$, and selecting the root that minimizes $J(\varepsilon)$, i.e.,

$$\hat{\varepsilon}=\arg\min_{\varepsilon\in\{\text{roots of P}\}}[J(\varepsilon)]. \tag{29}$$

Compared to the ML estimator, this third solution provides huge savings in the computational load. Simulations will later show that there is only a relatively modest accuracy degradation for small values of p due to the approximation made for $p<\frac{N}{2}$. As it has been said before, this simplified version will be used in the acquisition phase in order to provide a coarse estimation. Note that the second estimator of Eq. (25) can also provide a coarse estimation for $p<\frac{N}{2}$. But this estimation will be less accurate than the one provided by Eq. (29). The acquisition range of this algorithm is $\pm\frac{N}{2p}$ the subcarrier spacing, the same range as the first estimator.

3.4. Estimation Strategy

The carrier frequency offset estimation procedure is always divided into two phases; the acquisition phase which corresponds to coarse estimation and the tracking phase which refers fine adjustment.

If $p\geq\frac{N}{2}$, then there is not much to say, we will have only to use Eq. (25) which corresponds exactly to the ML estimate.

Since the estimation accuracy increases as the number of observations used for the estimation increases and as the length of observation vectors used here is $N-p$, then it is expected that by selecting small values of p, we will reach higher accuracy. For small values of p, using the ML estimator directly will induce a huge computational load since the search grid will be over $|\varepsilon|\leq\frac{N}{2p}$. Therefore, we propose to use the third estimator (or even the second estimator, if a smaller acquisition range is acceptable) in the acquisition phase in order to have a coarse estimation. This will insure that the residual CFO ε_r is small enough, i.e., $|\varepsilon_r|\leq\alpha$, where $\alpha\ll\frac{N}{2p}$. The first estimator can be then exploited to provide a very accurate estimation without involving a high computational load.

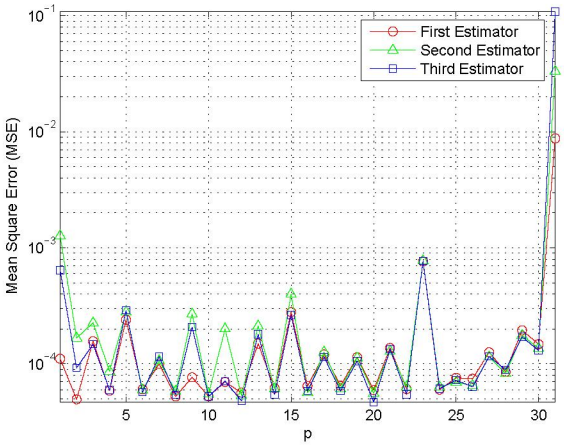

Fig. 1. Mean square error as a function of p, for N=32 and an AWGN channel with SNR=20 dB.

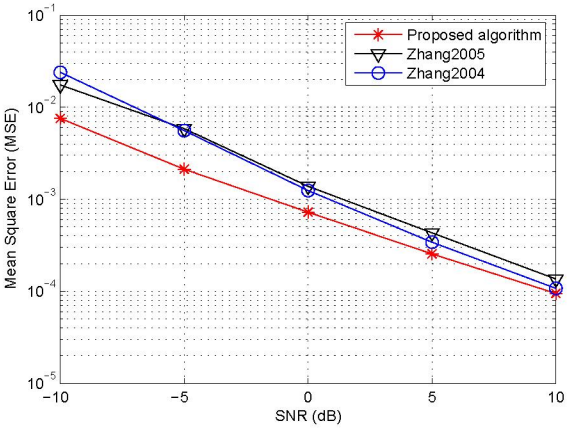

Fig. 2. Mean square error as a function of SNR in the multipath fading channel and $\varepsilon=0.01$.

4. NUMERICAL EXAMPLES

Fig.1 depicts the performance of the first, second and third estimators in Eq.(21), (25) and (29), respectively, for all values of p and a CFO fixed at 0.1, N set at 32 and an AWGN channel with 20 dB of SNR. 500 independent trials were performed for each value of p to obtain the mean-square error estimates. The search-grid resolution for the first estimator was set at 0.01 (55 points over the $\varepsilon\leq 0.55$ interval). For $p\geq\frac{N}{2}$, the three estimators give roughly the same estimation accuracy. This is as expected since the 3 estimators simply solve the same equation by 3 different means without making any different simplifying assumptions. When p is near $N-1$, the estimation accuracy of the three methods degrades. This can be explained by the fact that there will be few observations used for the estimation. For small values of p, the second and

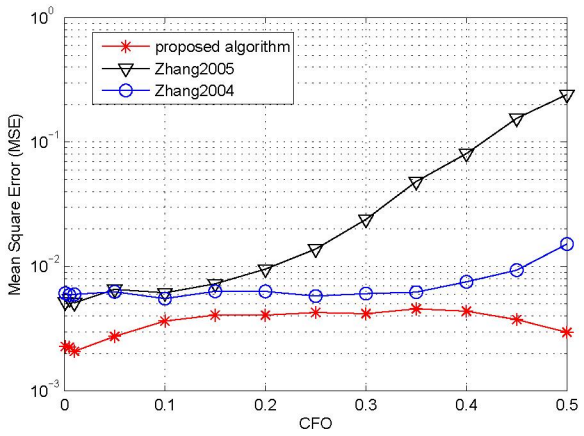

Fig. 3. MSE as a function of the CFO ($SNR = -5dB$).

third estimators give noticeably worst results compared to the first estimator. This is due to the fact that the approximations made to obtain these estimators are less exact for small values of p. But as p increases and tends toward $\frac{N}{2}$, the approximations become more and more accurate, and the three curves tend to overlap. One also can note that the estimation accuracy for even values of p is higher than the accuracy achieved for odd values of p. This is imputable to Eq. (11) that translates an approximation which is more accurate for even values of p than for odd values. But if we choose a greater value for N, this effect will be less noticeable.

In the following, we assume that the acquisition phase has been well performed and we will evaluate only the performance of the tracking phase using the first estimator. As a measure of performance in Fig.2, we have plotted the Mean Square Error (MSE) as a function of the SNR for our first estimator, and compared it with the methods proposed in [4] and [5], called here, respectively, Zhang2004 and Zhang2005. For fair comparisons, the three algorithms are tuned to achieve best performance, i.e., $p = 2$ for our algorithm, $\rho = 1$ for [5] and ($H_h = 7, H_l = 1$ and $L = 8$) for [4]. For this comparison, a system of 128 subcarriers was chosen with cyclic prefix length of 16. The CFO was fixed at 0.01, and 500 independent trials were performed. The simulations were conducted in a multipath environment having five paths with path delays of 0, 5, 9, 12 and 15 samples. The amplitude h_i of the ith path varies independently of the others according to a Rayleigh distribution with exponential power delay profile, i.e., $E[h_i^2] = exp(-\tau_i)$ where τ_i is the delay of the ith path.

From Fig.2 we can see that the proposed scheme clearly outperforms the two other techniques [4] and [5] (which have been proved to outperform the well known Schmidl's [2] and Morelli's [3] algorithms). At an MSE equal to 2×10^{-3}, the SNR gain is around 4 dB. For an SNR equal to 0 dB, the MSE is 7.25×10^{-4} for our algorithm and around 1.25×10^{-3} for the others schemes. At a relatively high SNR (around 10 dB), our algorithm and the one presented in [4] exhibit the same performance, but they are still superior to the one presented in [5].

Fig. 3 shows the MSE for different values of the CFO going from 0.001 to 0.5 at an SNR equal to -5 dB and for the same channel used previously. It can be seen that whatever the CFO value, the proposed algorithm has always a better accuracy. The estimation accuracy of the schemes [4] and [5] begins to degrade near $\varepsilon = 0.5$. This is imputable to the fact that the tracking algorithms there have, respectively, the following estimation ranges $|\varepsilon| < L/(2H_h)$ and $|\varepsilon| < N/(2(N-2))$ which translate here to $|\varepsilon| < 0.5714$ and $|\varepsilon| < 0.5079$.

5. CONCLUSION

In this paper, a new carrier frequency offset estimation scheme for OFDM has been presented. The estimation is based on the transmission of a specially designed synchronization symbol. The particular structure in the received samples of our synchronization symbol allows us to derive an ML-based estimator. This estimator can provide very high accuracy over a wide acquisition range. A simplified low-complexity version that can provide a coarse estimation was presented as an acquisition algorithm. Simulations have also proved that this new technique gives higher accuracy than the methods proposed in the literature.

6. REFERENCES

[1] T. Pollet, M. Van Bladel and M. Moeneclaey, "BER sensitivity of OFDM systems to carrier frequency offset and Wiener phase noise," *IEEE Trans. Commun.*, vol. 43, pp. 191-193, Feb./Mar./Apr. 1995.

[2] T. M. Schmidl and D. C. Fox, "Robust frequency and timing synchronization for OFDM," *IEEE Trans. Commun.*, vol. 45, pp. 1613-1621, Dec. 1997.

[3] M. Morelli and U. Mengali, "An improved frequency offset estimator for OFDM applications," *IEEE Communications Letters*, vol. 3, pp. 75-77, March. 1999.

[4] Z. Zhang, K. Long and Y. Liu, "Complex efficient carrier frequency offset estimation algorithm in OFDM systems," *IEEE Trans. Broadcasting*, Vol. 50, pp. 159-164, June 2004.

[5] Z. Zhang, K. Long and Y. Liu, "Joint frame synchronization and frequency offset estimationin OFDM systems," *IEEE Trans. Broadcasting*, Vol. 51, Sept. 2005.

[6] F.S. Acton, "Numerical Methods That Work," Mathematical Association of America, Washington, DC, pp. 331-334, 1990.